SEECCM III
3rd South-East European Conference on Computational Mechanics-
an ECCOMAS and IACM Special Interest Conference
M. Papadrakakis, M. Kojic, I. Tuncer, V. Papadopoulos (eds.)
Kos Island, Greece, 12–14 June 2013

A COMPUTATIONAL STUDY OF THE INJECTION THERAPY FOR MYOCARDIAL INFARCTION DURING THE NECROTIC STAGE

S. Skatulla[1], D. Legner[1], R.R. Rama[1], J. Mbewu[2], B. D. Reddy[2], N. Davies[3] and T. Franz[4]

[1]CERECAM, Department of Civil Engineering, University of Cape Town
7701 Rondebosch, Private Bag X3, South Africa
e-mail: {sebastian.skatulla,dieter.legner,riteshrao.rama}@uct.ac.za

[2]CERECAM, Department of Mathematics and Applied Mathematics
7701 Rondebosch, Private Bag X3, South Africa
e-mail: {daya.reddy,james.mbewu}@uct.ac.za

[3]CRVU, Chris Barnard Division of Cardiothoracic Surgery
7700 Mowbray, South Africa
e-mail: neil.davis@uct.ac.za

[4]CRVU, Chris Barnard Division of Cardiothoracic Surgery, University of Cape Town
PERC, Research Office, University of Cape Town
7701 Rondebosch, South Africa
Centre for High Performance Computing
7700 Rosebank, South Africa
e-mail: thomas.franz@uct.ac.za

Keywords: Myocardial Infarction, Injection Therapy, Computational Cardiology, Meshless Method.

Abstract. *Myocardial infarction is an increasing health problem worldwide. Due to an undersupply of blood, the cardiomyocytes in the affected region permanently lose their ability to contract. This in turn gradually weakens the overall heart function. A new therapeutic approach based on the injection of a gel into the infarcted area aims to support the healing and to inhibit adverse re-modelling that can lead to heart failure. A computational model is the basis for obtaining a better understanding of the heart mechanics, in particular, how myocardial infarction and gel injections affect its pumping performance. A strain invariant based stored energy function is proposed to account for the passive mechanical behaviour. The active contraction is represented by the Guccione model [1]. To incorporate injections an additive homogenization approach is introduced. The injectate has been characterized mechanically by indentation tests. As a numerical framework we are using the in-house code SESKA which is based on the Element-Free Galerkin method. The main focus of this contribution is to principally investigate how gel injections influence the mechanics and performance of the left ventricle during a full heart beat, i.e. in the diastolic filling and the systolic contraction phase. This investigation shows, that gel injections are able to reduce maximal fibre stresses caused by an infarct. This*

effect is dependent on the gel stiffness, whereas the higher the gel stiffness the more the diastolic filling is hampered, which is expected to influence pumping function as a side effect. A reduction of maximal fibre stresses is of importance with respect to prevent fatal rupture, which typically occurs during the necrotic phase. This might happen with preference in the highly stressed area, which based on the presented results can be found at the interface between infarct and healthy remote. The presence of stress peaks in that area is explained by the change of stiffness and contraction behaviour (contracting, non-contracting).

1 INTRODUCTION

Myocardial infarction, which constitutes a serious health problem, is a consequence of blockage of a coronary artery. Due to the resulting under-supply of oxygen, myocytes in the nearby region die. This in turn reduces the amount of contractile tissue and gradually weakens the overall heart function. Computational methods can be used to obtain a better understanding of how myocardial infarction affects cardiac function, and are therefore potentially useful in the design of suitable therapeutic treatments. A new therapeutic approach, which involves the injection of a gel into the infarcted heart, is the subject of this study.

Computational studies of the influence of injections into an infarcted heart were first carried out fairly recently. The usual approach to these problems has been the finite element method. WALL et al. [16] considered an infarcted ovine left ventricle (LV) and represented injections by modifying the material stiffness with regard to the healthy tissue. WENK et al. [18] primarily investigated the influence of polymeric injection patterns in a dog LV. In WENK et al. [17] an infarcted LV of a sheep and calcium hydroxiapatide-based injections were considered. KORTSMIT et al. [9] investigated the influence of polyethylene glycol-based hydrogel injections into an infarcted canine heart.

To reduce the complexity of the computational model most of the studies mentioned considered the left ventricle only. In WENK et al. [18] and NIEDERER et al. [11] the LV was idealized using an ellipsoidal geometry. Compared to the healthy remote, the infarcted tissue has to be described with different material properties. These change throughout the healing process (see for example GUPTA et al. [5], HOLMES et al. [7]). Research aimed at developing and optimizing injectable gels suitable to improve cardiac function has been initiated only recently (see NELSON et al. [10] for a good overview). A great variety of gels have been investigated: these range from biological to synthetic gels.

The present work focuses on the question of the potential of injection therapy and its effects in broad terms. Thus, instead of considering a realistic geometry of the left ventricle, a simplified ellipsoidal geometry which allows the fibre directions to be described in terms of prolated ellipsoidal coordinates is used (see also WENK et al. [18], NIEDERER et al. [11]).

The structure of the present contribution is as follows: In section 2 the constitutive models relevant to cardiac mechanics in this work are discussed. In section 3 the numerical model is described, benchmarked, and subsequently used to investigate healthy, infarcted and injected left ventricles. The results are presented in section 4 for diastolic filling and systolic isovolumetric contraction. Finally, section 5 concludes the work by briefly evaluating the applicability of the present model, the innovative aspects, and the findings. The section closes with comments on potential future investigations.

2 Constitutive modelling

2.1 Passive stress model

Passive behaviour in the left ventricle wall is modelled as as a nonlinear, orthotropic and nearly incompressible hyperelastic material, with strain energy function

$$W = A(e^{Q} - 1)/2 + A_{\text{compr}} \left\{ \det[\mathbf{U}] \, \ln(\det[\mathbf{U}]) - \det[\mathbf{U}] + 1 \right\} \quad . \tag{1}$$

Here, Q given by

$$Q = b_{11}\hat{E}_{11}^2 + b_{22}\hat{E}_{22}^2 + b_{33}\hat{E}_{33}^2 + b_{12}(\hat{E}_{12}^2 + \hat{E}_{21}^2) + b_{13}(\hat{E}_{13}^2 + \hat{E}_{31}^2) + b_{23}(\hat{E}_{23}^2 + \hat{E}_{32}^2) \tag{2}$$

(see USYK et al. [15]). The components $\hat{E}_{ij}$ of the *Green* strain $\mathbf{E}$ are relative to a local orthonormal basis $\mathbf{V}_i$ with fibre axis $\mathbf{V}_1$, sheet axis $\mathbf{V}_2$, and sheet-normal axis $\mathbf{V}_3$:

$$\begin{aligned} \mathbf{E} &= \hat{E}_{11}\mathbf{V}_1 \otimes \mathbf{V}_1 + \hat{E}_{22}\mathbf{V}_2 \otimes \mathbf{V}_2 + \hat{E}_{33}\mathbf{V}_3 \otimes \mathbf{V}_3 + \hat{E}_{12}(\mathbf{V}_1 \otimes \mathbf{V}_2 + \mathbf{V}_2 \otimes \mathbf{V}_1) \\ &+ \hat{E}_{13}(\mathbf{V}_1 \otimes \mathbf{V}_3 + \mathbf{V}_3 \otimes \mathbf{V}_1) + \hat{E}_{23}(\mathbf{V}_2 \otimes \mathbf{V}_3 + \mathbf{V}_3 \otimes \mathbf{V}_2) \quad . \end{aligned} \tag{3}$$

The right stretch tensor is denoted by $\mathbf{U}$. Then Q may be expressed in the form

$$\begin{aligned} Q &:= a_1(\mathrm{tr}(\mathbf{M}^1\mathbf{E}))^2 + \mathrm{a}_2(\mathrm{tr}(\mathbf{M}^2\mathbf{E}))^2 + \mathrm{a}_3(\mathrm{tr}(\mathbf{M}^3\mathbf{E}))^2 \\ &+ a_4\mathrm{tr}(\mathbf{M}^1\mathbf{E}^2) + \mathrm{a}_5\mathrm{tr}(\mathbf{M}^2\mathbf{E}^2) + \mathrm{a}_6\mathrm{tr}(\mathbf{M}^3\mathbf{E}^2) \quad , \end{aligned} \tag{4}$$

with the structural tensors $\mathbf{M}^i$ defined by

$$\mathbf{M}^1 = \mathbf{V}_1 \otimes \mathbf{V}_1 \quad , \quad \mathbf{M}^2 = \mathbf{V}_2 \otimes \mathbf{V}_2 \quad , \quad \mathbf{M}^3 = \mathbf{V}_3 \otimes \mathbf{V}_3 \quad . \tag{5}$$

Now the orthotropic constitutive model is used to represent transversely isotropic behaviour of the heart wall. Following OMENS et al. [12] and NIEDERER et al. [11] for the rat LV we use the set of material coefficients given in Tab. 1. A comparison of eq. 2 and eq. 4 yields

b_{11}	b_{22}	b_{33}	b_{12}	b_{13}	b_{23}
9.2	2.0	2.0	3.7	3.7	1.0

Table 1: Material coefficients used in the strain energy function eq. 1, eq. 2

the parameters for the strain invariant formulation in Tab. 2. The coefficients A and A_{compr}

a_1	a_2	a_3	a_4	a_5	a_6
2.8	1.0	1.0	6.4	1.0	1.0

Table 2: Material coefficients used in the strain invariant representation eq. 1, eq. 4

are determined by calibrating the numerical model of the left ventricle of the rat, as will be described later.

2.2 Active stress model

In the active stress formulation the sum of a passive stress $\mathbf{S}_P$ representing the passive mechanical response of tissue to loads and an active contractile stress $\mathbf{S}_A$ defines the total stress

$$\mathbf{S} = \mathbf{S}_P + \mathbf{S}_A \quad . \tag{6}$$

The passive stress is obtained from the passive mechanical constitutive law, so that when there is no active stress ($\mathbf{S}_A = \mathbf{0}$), the myocardium simply behaves passively. The active stress acts in the direction of the fibre $\mathbf{V}_1$; that is,

$$\mathbf{S}_A = T_A\, \mathbf{V}_1 \otimes \mathbf{V}_1 \quad . \tag{7}$$

The variable T_A represents the active tension developed in the myocyte and is derived from a cellular model of tension development in myocytes. For the purpose of studying the tissue-level mechanics of the heart the model of GUCCIONE et al. [4] is adopted. This model was

derived from biophysical considerations of calcium dynamics and crossbridge formation. The parameters used in the model were calibrated to fit experimental tension test data of a dog, while the magnitude of the active tension was modified to represent that of a rat. The Guccione model predicts the tension according to

$$T_A = T_{\max} \frac{Ca_0^2}{Ca_0^2 + ECa_{50}^2(l)} C_t(l,t) \tag{8}$$

where C_t represents the time transient, a function of time and sarcomere length, ECa_{50}^2 represents the calcium concentration at 50% tension, Ca_0 is the peak intracellular calcium concentration, l is the sarcomere length, and $T_{\max}$ is the maximum tension developed. The functions C_t and ECa_{50} are given by

$$C_t = \tfrac{1}{2}\left(1 - \cos\omega(l,t)\right) \quad , \tag{9}$$

$$ECa_{50}(l) = \begin{cases} \frac{Ca_0^{\max}}{\sqrt{\exp[B(l-l_0)]-1}} & \text{for } l > l_0 \quad , \\ 0 & \text{for } l \leq l_0 \quad , \end{cases} \tag{10}$$

where t_0 is the time at maximum tension, B is a constant and l_0 is the sarcomere length below which there is no active tension developed. The sarcomere length is a function of the stretch with respect to the reference configuration in the fibre direction so that

$$l = l_R \sqrt{2\mathrm{tr}\left((\mathbf{V}_1 \otimes \mathbf{V}_1)\mathbf{E}\right) + 1} = l_R \sqrt{2E_{\mathrm{ff}} + 1} \tag{11}$$

where l_R is the sarcomere rest length in the undeformed reference configuration and E_{ff} the direct component of *Green* strain in the fibre direction. The time-dependence of the active tension is described by

$$\omega(l,t) = \begin{cases} \pi \frac{t}{t_0} & \text{for } 0 \leq t < t_0 \quad , \\ \pi \left[\frac{t-t_0}{t_r(l)} + 1\right] & \text{for } t_0 \leq t < t_0 + t_r \quad , \\ 0 & \text{for } t \geq t_0 + t_r \quad , \end{cases} \tag{12}$$

which also takes into account the influence of the current sarcomere length on the duration of active contraction, that is, the length-dependence of the calcium sensitivy of proteins that cause tension development. The constant t_0 is the time to peak tension and t_r is the duration of the relaxation period described as a function of the sarcomere length

$$t_r = m \cdot l + b \tag{13}$$

with constants m and b. The parameters used in the Guccione model are given in Tab. 3.

$T_{\max}$ [kPa]	Ca_0 [μM]	$Ca_0^{\max}$ [μM]	B [$\frac{1}{\mu\mathrm{m}}$]	l_0 [μm]	t_0 [ms]	m [$\frac{s}{\mu\mathrm{m}}$]	b [ms]
56.7	4.35	4.35	4.75	1.58	250	1.0489	-1429

Table 3: Parameters used in Guccione model.

2.3 Homogenization approach

The infarcted and injected myocardial tissue is modelled as an homogenized, that is, averaged, material response. Similar approaches can be found for the case of elasticity in REESE et al. [13] or for elasto-plasticity in KLINKEL et al. [8]. Considering hyperelastic material behaviour, we introduce a stored energy function of the form

$$\psi = \sum_{I=1}^{m} n_I \, \psi_I \left(\mathbf{E} \right) \tag{14}$$

where m denotes the number of superimposed material phases and n_I, $I = 1, m$ the corresponding volume fractions associated with the stored energy functions ψ_I, each representing the material behaviour of a specific constituent. The weighted nature of the overall response is achieved by imposing the constraint $\sum_{I=1}^{m} n_I = 1$. The different material phases are linked by the kinematic constraint that the deformation gradient applies to all of them. Consequently, the averaged second *Piola-Kirchhoff* stress tensor is given by

$$\mathbf{S} \;=\; \frac{\partial \psi}{\partial \mathbf{E}} = \sum_{I=1}^{m} n_I \, \frac{\partial \psi_I}{\partial \mathbf{E}} \quad . \tag{15}$$

In particular, the healthy myocardium consists of one single active anisotropic phase, and the injected infarct region consists of two passive phases, an anisotropic and an isotropic one, the latter for the injected biogel. In this sense, at each point the stress response of the mixture as well as of each individual component can be obtained. The latter is useful, as the influence of the biogel, in terms of amount of injectate and stiffness, on the fibre stress experienced in the infarct area is of special interest.

3 Numerical model

In this section the numerical model for the healthy LV is first described and benchmarked by comparison with data from the literature. Secondly, the model is used to study the effect of the new therapeutic method on the idealized infarcted ventricle. More specifically, an infarcted left ventricle of a rat during diastolic filling and systolic isovolumetric contraction is considered. Fatal wall rupture commonly occurs in the necrotic phase, as stresses are elevated due to a increase in stiffness of the infarct tissue as well as wall thinning due to removal of dead tissue at that stage. Earlier infarct stages are commonly reserved for medicamentous or surgical treatment to dissolve or bypass the blockade. Later healing stages and remodelling are strongly influenced by boundary conditions which are set in the necrotic healing stage, e.g. see HOLMES et al. [7]. Thus, this contribution focuses on the impact of gel injections into the infarcted area during the necrotic healing phase.
An overlapping of the injectate into the border zone between infarct and healthy remote is considered. For the infarct stage it is assumed that the remaining healthy tissue within the border zone maintains its contractile properties. It is assumed further that the removed volume of dead tissue for both the infarct area and the border zone is in balance with the injectate volume. As the constitutive behaviour of the border zone for the different healing stages is still under scientific discussion, such an assumption does not represent reality. Nevertheless, it allows the phenomenology of the border zone and the essential aspects of injections to be captured in a general sense, in line with the purpose of this investigation. The area between the healthy remote and infarct (injection) region is referred to as the overlap zone.

	healthy zone	infarct zone	overlap zone
healthy (a)	$100\,\%$	$0\,\%$	$0\,\%$
infarcted (b)	$84.2\,\%$	$15.8\,\%$	$0\,\%$
injected (c)	$71.0\,\%$	$15.8\,\%$	$13.2\,\%$

Table 4: Volume fractions with respect to the total wall volume for (a) healthy, (b) infarcted, (c) injected case

3.1 Truncated ellipsoidal model of the rat left ventricle

The geometry of the left ventricle is assumed to be described by a truncated ellipsoid. This may conveniently be described in terms of prolate spheroidal coordinates (ξ, η, θ) which are related to the Cartesian ones (x, y, z) by

$$\begin{aligned} x &= C \cdot \sinh(\xi) \cdot \sin(\eta) \cdot \cos(\theta) \\ y &= C \cdot \sinh(\xi) \cdot \sin(\eta) \cdot \sin(\theta) \\ z &= C \cdot \cosh(\xi) \cdot \cos(\eta) \qquad . \end{aligned} \tag{16}$$

In accordance with NIEDERER et al. [11] the endocardial and epicardial radii at the widest point are $2.4\,\mathrm{mm}$ and $5.1\,\mathrm{mm}$, respectively. The distance from the apex to the base is $11.5\,\mathrm{mm}$ for the endocardium (endo) and $13.2\,\mathrm{mm}$ for the epicardium (epi). This corresponds to $\xi_{endo} = 0.31$, $\xi_{epi} = 0.60$ and the focal lengths $C_{endo} = 7.61\,\mathrm{mm}$, $C_{epi} = 8.01\,\mathrm{mm}$. It follows that $V_{cav}^{init} = 155.57\,\mu\mathrm{l}$ and $V_{myo}^{init} = 641.96\,\mu\mathrm{l}$ for the initial cavity volume and the initial myocardial wall volume, respectively. The varying fibre directions throughout the wall are adopted from RIJCKEN et al. [14]. With respect to the geometric boundary conditions the natural deformation of the LV during a heartbeat shows that almost the whole LV undergoes vertical, horizontal and transversal movements simultaneously. Only the movement of the base is restricted. Hence, the endocardial ring is fixed at the base and the surface displacement of the base is restrained in the vertical direction.

3.2 Model calibration

The numerical model of the healthy left ventricle is calibrated by using pressure-volume relations given in the literature. In combination with the parameters given in Tab. 2 the coefficients $A = 1.00\,\mathrm{kPa}$ and $A_{compr} = 300.00\,\mathrm{kPa}$ are chosen (see eq. 1), to adjust the passive stress model as discussed in section 2.1. With this choice the relation between cavity volume and increasing cavity pressure applied to the endocardial wall of the present numerical model agrees well with results reported in the recent literature: see Fig. 1. Furthermore, for the cavity pressure $p_{cav} = 30.0\,\mathrm{mmHg}$ the calculated myocardial wall volume $V_{myo} = 639.98\,\mu\mathrm{l}$ is still very close to the initial one $V_{myo}^{init} = 641.96\,\mu\mathrm{l}$, hence the myocardial wall behaves nearly isochorically.

3.3 Case study

We distinguish three cases: (a) a healthy LV; (b) an infarcted LV; and (c) infarcted and injected LV (see Fig. 2). The relevant volume fractions for these three cases can be found in Tab. 4, where with respect to the grading given in WENK et al. [19] an infarct of grade 1 ($< 20\%$) is considered here. A fatal rupture of the infarct tissue generally occurs during the necrotic phase. This motivates the consideration of an infarct at that healing stage, and the investigation of the influence of a hydrogel injection directly into the infarct zone (red). To represent the fact that the hydrogel injection stops abrubtly at the infarct border, we consider a so-called overlap zone

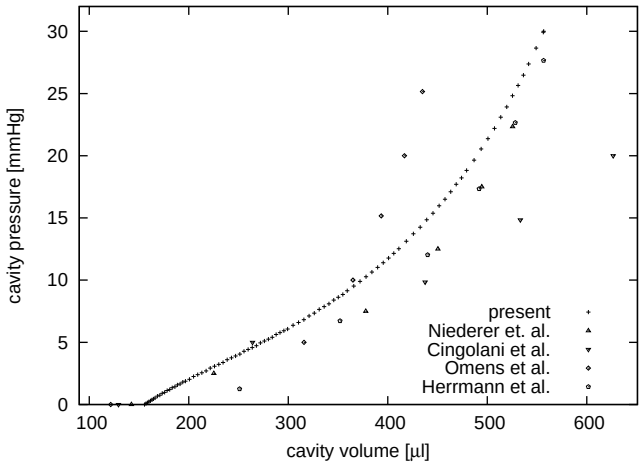

Figure 1: Pressure-volume relation for the left ventricle using the present model compared with data from NIEDERER et al. [11], CINGOLANI et al. [3], OMENS et al. [12], HERRMANN et al. [6]

(grey) into the healthy remote (blue). In order to model a smooth transition the overlap zone has a reduced gel volume fraction compared to the gel volume fraction of the infarct area. The infarct zone and overlap zone are incorporated by intersecting the truncated ellipsoid with two spheres of different radii. To represent the stiffening of the infarct tissue during the necrotic

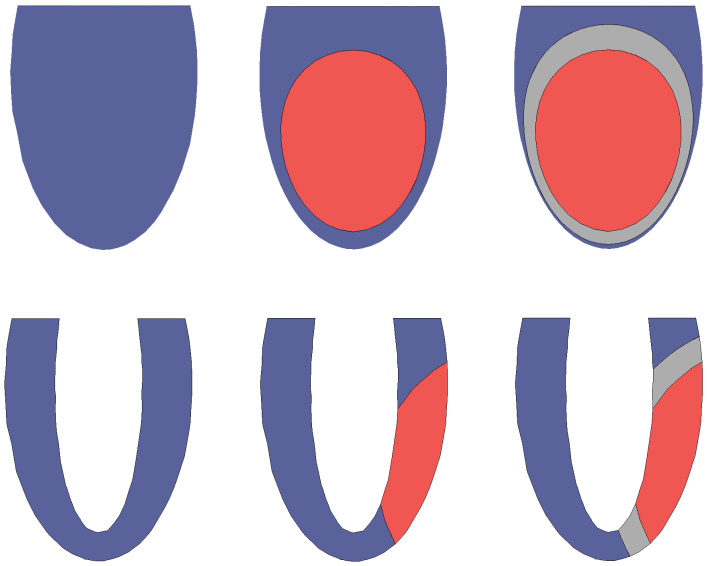

Figure 2: Front view (top row) and vertical cut (bottom row) of the (a) healthy, (b) infarcted, (c) injected LV with healthy remote (blue), infarct (red) and overlap zone (grey)

stage of healing considered here (see for example GUPTA et al. [5], HOLMES et al. [7]), the infarct stiffness is set at twice that of the healthy remote. That is, the weighting factor in the passive stress model is $A = 2.00\,\mathrm{kPa}$, see eq. 1. Based on unpublished experiments and characterization procedures, the hydrogel compound is approximated by a Neo-Hookean material model with the material parameters $\mu = 24.6\,\mathrm{Pa}$ and $\lambda = 983.6\,\mathrm{Pa}$, which are from now on referred to collectively using the notation kgel. We subdivide the injection case (c) into four cases (c1), (c2), (c3), (c4), referring respectively to 0.25 kgel, 0.50 kgel, 0.75 kgel, 1.0 kgel. Hereby, (c4) represents the actual hydrogel, whereas (c1) - (c3) are hypothetical injectates with

reduced stiffness. That is μ and λ of (c4) given above are multiplied by the factor 0.25, 0.50 and 0.75, respectively. To account for the wall-thinning effect, in case (b) the infarct volume contains 90% infarct material and 10% of a dummy material with negligible stiffness, representing the dead material transported away at the micro-structural level. The hydrogel-treated infarct region, case (c), is made up of a homogenized mixture of infarct and hydrogel material. Basically, the volume of the injectate in that case replaces the dummy material of case (b). The overlap zone is modelled with 95% healthy tissue and 5% hydrogel. This mixture ratio reflects the assumption that the injectate enters the healthy tissue surrounding the infarct within a limited radius, referred to as the overlap zone. The mixing of materials is achieved by employing the homogenization approach discussed in section 2.3.

4 Numerical results

The results for the healthy (a), infarcted (b) and injected (c1) - (c4) cases are now shown separately for diastolic filling and systolic isochoric contraction. During diastolic filling the cavity pressure p_{cav} is increased up to $p_{\text{cav}}^{\text{EDF}} = 7.5\,\text{mmHg}$, marking the end of the diastolic filling phase. At the outset of the systolic isovolumetric contraction phase the active stress model of section 2.2 is initiated and the cavity pressure is increased up to a value $p_{\text{cav}}^{\text{ESIC}} = 37.5\,\text{mmHg}$ while the cavity volume is enforced to be constant. The pressure values $p_{\text{cav}}^{\text{EDF}}$ and $p_{\text{cav}}^{\text{ESIC}}$ for the rat left ventricle are adopted from NIEDERER et al. [11]. The computational model is developed using the element-free Galerkin method (see for example BELYTSCHKO et al. [1]), implemented in the in-house code *SESKA*. The numerical model of the left ventricle consists of 1700 particles. It was found that further refinements did not lead to any significant change in the results.

4.1 Diastolic filling

Comparing the healthy case (a) with the infarct case (b) in Fig. 3, an overall reduction in cavity volume is observed during diastolic filling, which indicates that the overall infarct stiffness is increased in the necrotic healing stage. This is reasonable and is also reported in the literature, for example by BOGEN et al. [2], HOLMES et al. [7], as the resulting infarct stiffness takes into account two kinds of effects: (i) a slight reduction in stiffness as a portion of dead myocytes has been transported away leading to a lower material density on micro-structural level and thus, a reduced effective wall thickness; (ii) a significant increase of stiffness of the remaining infarcted myocardium GUPTA et al. [5]. The homogenized, i.e. averaged, stiffness in the infarct zone is consequently higher than in the healthy remote, explaining the reduction in LV compliance. For all injectates (c1) - (c4), the end-diastolic cavity volume is predicted to be smaller than in case (a) and (b), see Fig. 3, which indicates that the injectate (c4) is fairly stiff. Even the hypothetically considered injectates (c1) - (c3) with reduced stiffness hamper diastolic filling considerably.

This finding is confirmed by the deformation results obtained at the end of diastolic filling $p_{\text{cav}}^{\text{EDF}}$, shown in terms of a representative vertical cut in Fig. 4 for all cases considered. A qualitative comparison with the undeformed configuration, see Fig. 2, reveals that the infarct and injectate stiffnesses are inversely related to the wall thickness reduction in the respective regions for cases (b) - (c). The deformation behaviour in the healthy remote is similar for all the cases (a) - (c). We consider next the myocardial fibre stress and effective strain, and compare qualitatively the mechanical response for the cases considered.

Fig. 5 shows no significant increase in end-diastolic tissue fibre stress for the infarcted case (b).

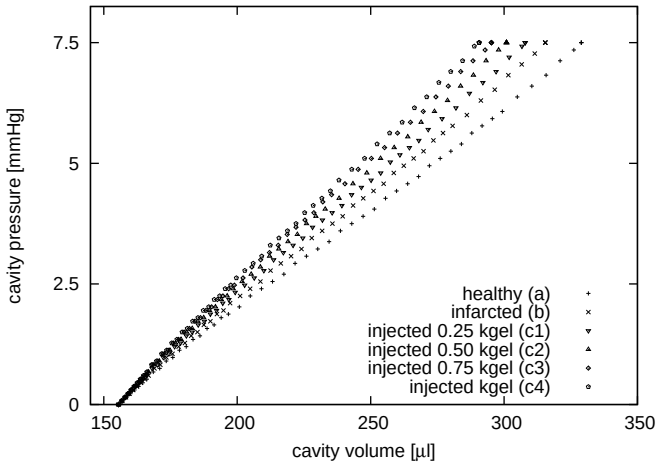

Figure 3: Pressure-volume relations during diastolic filling of healthy (a), infarcted (b), injected (c1) - (c4) left ventricle

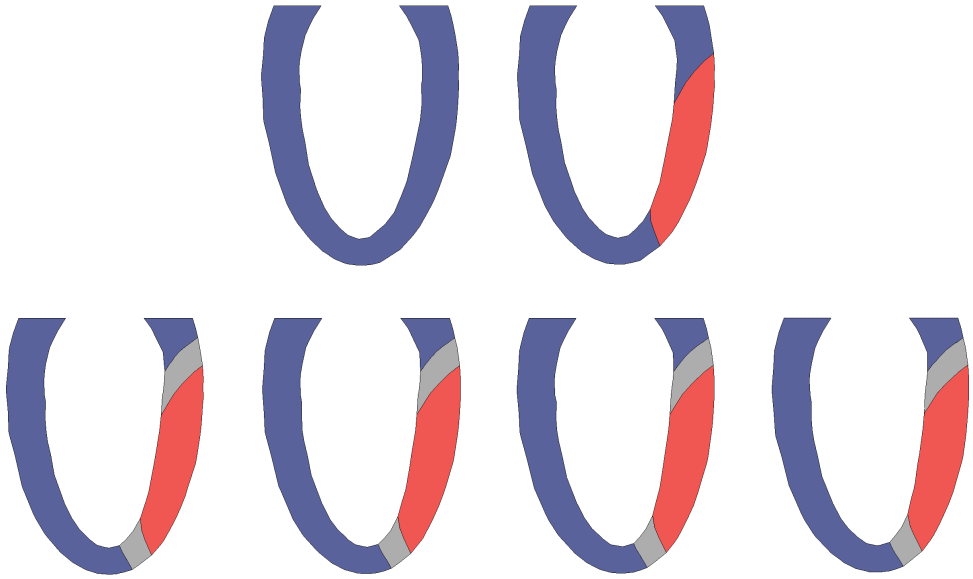

Figure 4: Deformation of the left ventricle at the end of diastolic filling - top row: (a) healthy (left), (b) infarcted (right); bottom row: injected (c1), (c2), (c3), (c4) from left to right

However, it can be seen that the stiffer the injectate in cases (c1) - (c4), the greater the reduction in the tissue fibre stresses compared to healthy case (a) and infarcted case (b), respectively. This is explained by the fact that a stiffer injectate has a reinforcing effect and thus reduces the myocardial fibre stress.
Fig. 6 shows that the effective strains are clearly reduced due to the higher stiffness of the infarct case (b), and are even further reduced when hydrogel is injected, as in cases (c1) - (c4). This observation is confirmed by studying the pressure-volume relation Fig. 3 and the deformed cross-sections Fig. 4, which indicates a decrease in filling compliance.

4.2 Systolic isovolumetric contraction

In contrast to the diastolic filling phase, the left ventricle during the systolic isovolumetric phase is subjected to active contraction at constant cavity volume, causing an increase in cavity

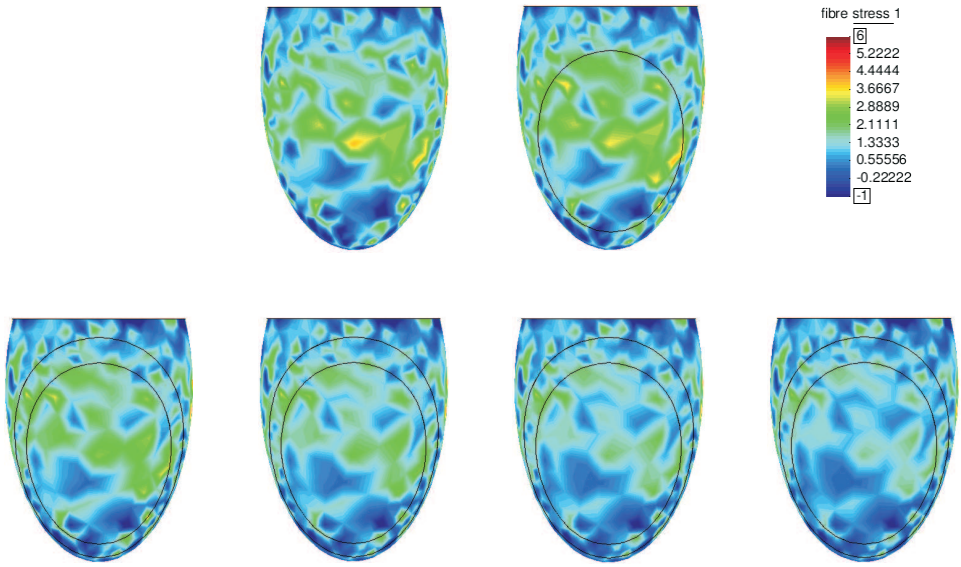

Figure 5: Fibre stress distribution at the end of diastolic filling - top row: (a) healthy (left), (b) infarcted (right); bottom row: injected (c1), (c2), (c3), (c4) from left to right

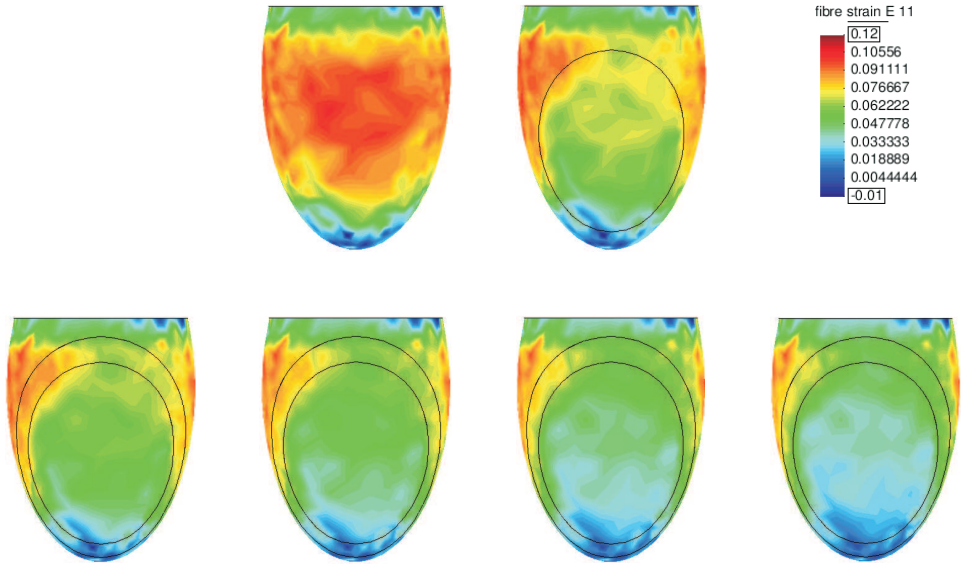

Figure 6: Distribution of strain in fibre direction at the end of diastolic filling - top row: (a) healthy (left), (b) infarcted (right); bottom row: injected (c1), (c2), (c3), (c4) from left to right

pressure. Qualitatively, the resulting deformation at the end of systolic isovolumetric contraction depicted in Fig. 7 shows a slight vertical elongation accompanied by a wall-thickness reduction as compared with the configuration at end-diastolic filling in Fig. 4. This feature of the deformation correlates with the constant cavity volume during isovolumetric contraction and the almost incompressible constitutive modeling of the LV wall. In accordance with NIEDERER et al. [11] longitudinal shortening and an increase in wall thickness is only to be expected for systolic ejection, which is not considered in the framework of this contribution. Compared to the diastolic phase the deformation in cases (b) and (c) occurs in a less symmetric way than for the diastolic phase. Fig. 8 illustrates on the one hand drastically reduced fibre stresses within the infarcted region for the untreated infarct case (b) and the injected infarct cases (c1) - (c4) compared to the healthy case (a). On the other hand it can be observed that at the interface

between the healthy and infarcted area in case (b) the maximal fibre stresses are greater than for the healthy case (a). Studying the injected cases (c1) - (c4), it can be seen that the injection relieves this highly stressed zone of case (b) even below healthy levels, whereas the stiffness of the injectate is without major influence. Due to the loss of active contraction the infarcted region is almost completely subjected to stretch, see Fig. 9. This feature can also be observed for all injection cases.

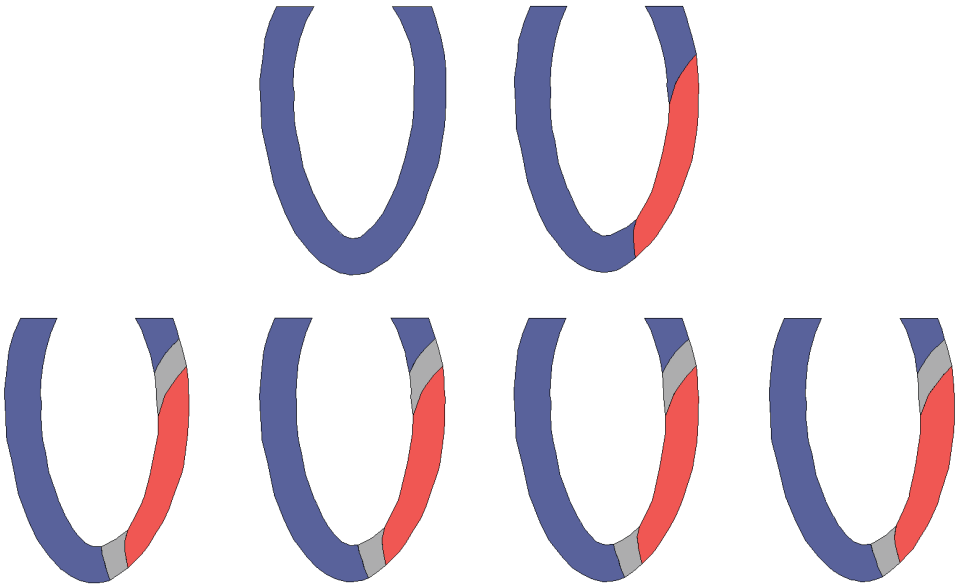

Figure 7: Deformation of the left ventricle at the end of isovolumetric systolic contraction - top row: (a) healthy (left), (b) infarcted (right); bottom row: injected (c1), (c2), (c3), (c4) from left to right

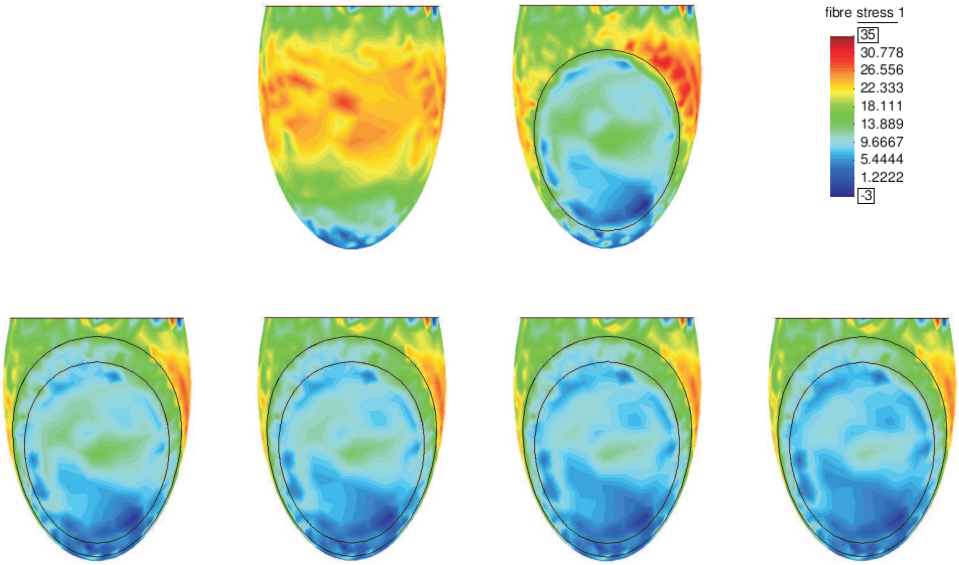

Figure 8: Fibre stress distribution at the end of isovolumetric systolic contraction - top row: (a) healthy (left), (b) infarcted (right); bottom row: injected (c1), (c2), (c3), (c4) from left to right

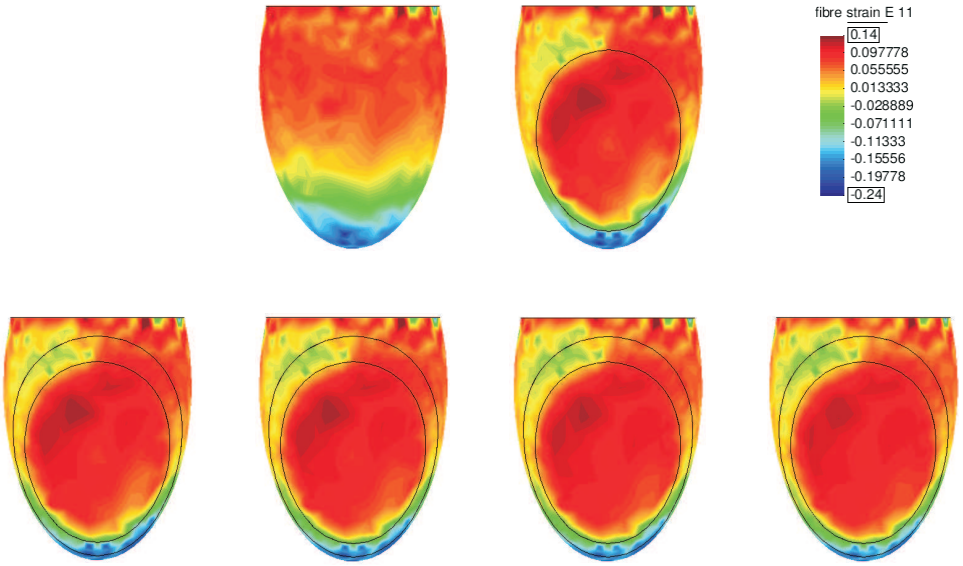

Figure 9: Distribution of strain in fibre direction at the end of isovolumetric systolic contraction - top row: (a) healthy (left), (b) infarcted (right); bottom row: injected (c1), (c2), (c3), (c4) from left to right

5 Conclusion

5.1 The applicability of the model

The objective of the present investigation is not to provide definitive, quantitative results for a realistic LV. Instead, the focus of the contribution has been to study qualitatively the influence of hydrogel injections into an infarcted left ventricle, modelled by a geometry that is simple yet able to capture key features. Of particular interest are representative values for the pressure, volume, deformation, and stress and strain quantities. In this regard, for the sake of simplicity a rotational symmetric geometry is used and an overlap zone representing a more realistic gel distribution is considered. Further, the active contraction is simultaneously initiated throughout the LV. Attention is restricted to the necrotic healing phase by considering a grade 1 infarct, with the assumption that the amount of injectate is equal to the amount of removed tissue for both the infarct and the overlap zone.

5.2 Novel aspects of this contribution

A meshless method is used as the basis for the numerical model and simulations. A strain invariant-based stored energy function is introduced, allowing frame-invariant and more compact expressions for the stress tensors and material tensors. A homogenization approach is introduced to account for representative material behaviour of an arbitrary mix of different materials and volume fractions. Four different injection types are investigated and compared with the healthy and infarcted case, where one of them is a realistic gel which is being used in current experiments.

5.3 Findings

This investigation shows that gel injections are able to reduce maximal fibre stresses caused by an infarct. The higher the gel stiffness the more the diastolic filling is hampered, which is expected to influence pumping function as a side effect. A reduction of maximal fibre stresses is of importance with respect to the prevention of fatal rupture, which typically occurs during

the necrotic phase. This could be more likely in the highly stressed area, which on the basis of the results presented can be found at the interface between the infarct and healthy remote. The presence of stress peaks in that area is explained by the discontinuity of stiffness and contraction behaviour (contracting, non-contracting).

5.4 Recommendations / Outlook

It would be of interest to investigate he effects of injections only at the interface zone, thus providing a smoother transition of mechanical properties. As such a strategy would also reduce the amount of injectate, and the net reduction of overall pumping function might be less pronounced, which could be confirmed, for example, in terms of monitoring typical cardiac parameters like stroke volume, ejection fraction, etc. Nevertheless, with respect to later healing stages the injection modalities that account, for example, for weaker infarct stiffness causing thinning of the infarct zone itself, followed by negative remodeling of the LV might be different. Thus, the timing of the injections and the chosen injectate degradabilities are other important aspects for future investigations, within a dynamic context, to contribute to a more complete understanding and assessment of the therapeutic suitability of the gel.

5.5 Acknowledgement

The research leading to this work has been supported by the Centre for High Performance Computing of South Africa. The financial support of the Claude Leon Foundation through a postdoctoral fellowship for D.L. is gratefully acknowledged. B.D.R. acknowledges the support of the National Research Foundation through the South African Research Chair in Computational Mechanics.

References

[1] T. Belytschko, Y. Krongauz, D. Organ, M. Fleming, and P. Krysl. Meshless methods: An overview and recent developments. *Comput. Methods Appl. Mech. Engrg.*, 139:3–47, 1996.

[2] D.K. Bogen, S.A. Rabinowitz, A. Needleman, T.A. McMahon, and W. H. Abelmann. An analysis of the mechanical disadvantage of myocardial infarction in the canine left ventricle. *Circulation Research*, 47:728–41, 1980.

[3] O.H. Cingolani, X.P. Yang, M.A. Cavasin, and O. A. Carretero. Increased systolic performance with diastolic dysfunction in adult spontaneously hypertensive rats. *Hypertension*, 43:249–254, 2003.

[4] J. M. Guccione, L. K. Waldman, A. D. McCulloch, et al. Mechanics of active contraction in cardiac muscle: Part ii–cylindrical models of the systolic left ventricle. *Journal of biomechanical engineering*, 115(1):82, 1993.

[5] K. B. Gupta, M. B. Ratcliffe, M. A. Fallert, L. H. Edmunds, and D. K. Bogen. Changes in passive mechanical stiffness of myocardial tissue with aneurysm formation. *Circulation*, 89:2315–2326, 1994.

[6] K. L. Herrmann, A. D. McCulloch, and J. H. Omens. Glycated collagen cross-linking alters cardiac mechanics in volume-overload hypertrophy. *Am J Physiol Heart Circ Physiol*, 284:1277–1284, 2003.

[7] J. W. Holmes, T. K. Borg, and J. W. Covell. Structure and mechanics of healing myocardial infarcts. *Annual Review of Biomedical Engineering*, 7:223–253, 2005.

[8] S. Klinkel, C. Sansour, and W. Wagner. An anisotropic fibre-matrix material model at finite elastic-plastic strains. *Computational Mechanics*, 35:409–417, 2005.

[9] J. Kortsmit, N.H. Davies, R. Miller, J.R. Macadangdang, P. Zilla, and T. Franz. The effect of hydrogel injection on cardiac function and myocardial mechanics in a computational post-infarction model. *Computer Methods in Biomechanics and Biomedical Engineering*, 2012.

[10] D M Nelson, Z Ma, K L Fujimoto, R Hashizume, and W R Wagner. Intra-myocardial biomaterial injection therapy in the treatment of heart failure: Materials, outcomes and challenges. *Acta Biomaterialia*, 7:1–15, 2011.

[11] S.A. Niederer and N.P. Smith. The role of the frankstarling law in the transduction of cellular work to whole organ pump function: A computational modeling analysis,. *PLoS Comput Biol*, 5:1–5, 2009.

[12] Jeffrey H. Omens, Deidre A. MacKenna, and Andrew D. McCulloch. Measurement of strain and analysis of stress in resting rat left ventricular myocardium. *Journal of Biomechanics*, 26:665–676, 1993.

[13] S. Reese, T. Raible, and P. Wriggers. Finite element modelling of orthotropic material behaviour in pneumatic membranes. *International Journal of Solids and Structures*, 52: 9525–9544, 2001.

[14] J. Rijcken, P. H. Bovendeerd, A. J. Schoofs, D. H. van Campen, and T. Arts. Optimization of cardiac fiber orientation for homogeneous fiber strain during ejection. *Ann Biomed Eng*, 27(3):289–97, 1999.

[15] T.P. Usyk, R. Mazhari, and A.D. McCulloch. Effect of laminar orthotropic myofiber architecture on regional stress and strain in the canine left ventricle. *Journal of Elasticity*, 61:143–164, 2000.

[16] Samuel T Wall, Joseph C Walker, Kevin E Healy, Mark B Ratcliffe, and Julius M Guccione. Theoretical impact of the injection of material into the myocardium. *Circulation*, 114:2627–2635, 2006.

[17] J. F. Wenk, P. Eslami, Z. Zhang, C. Xu, E. Kuhl, J.H. Gorman III, J.D. Robb, Ratcliffe M.B., R.C. Gorman, and J.M. Guccione. A novel method for quantifying the in-vivo mechanical effect of material injected into a myocardial infarction. *Ann Thorac Surg*, 92: 935–941, 2011.

[18] J.F. Wenk, S.T. Wall, R.C. Peterson, S.L. Helgerson, H.N. Sabbah, M. Burger, N. Stander, M.B. Ratcliffe, and J.M. Guccione. A method for automatically optimizing medical devices for treating heart failure: designing polymeric injection patterns. *Journal of biomechanical engineering*, 131:121011, 2009.

[19] J.F. Wenk, Z. Zhang, G. Cheng, D. Malhotra, G. Acevedo-Bolton, M. Burger, T. Suzuki, D. A. Saloner, W. Wallace, J. Guccione, and M.B. Ratcliffe. First finite element model of the left ventricle with mitral valve: Insights into ischemic mitral regurgitation. *Ann Thorac Surg*, 89:1546–1554, 2010.